Applied Catalysis A: General 499 (2015) 13–18

Contents lists available at ScienceDirect

Applied Catalysis A: General

journal homepage: www.elsevier.com/locate/apcata

Catalytic performance of Ni/La_2O_3 materials in glycerol valorization for acetol and syngas production

Diana Hernández, Diana López, Jhon J. Fernández*

Grupo Química de Recursos Energéticos y Medio Ambiente, Instituto de Química, Facultad de Ciencias Exactas y Naturales, Universidad de Antioquia (UdeA), Calle 70 No. 52-21, Medellín, Colombia

ARTICLE INFO

Article history:
Received 1 December 2014
Received in revised form 28 March 2015
Accepted 30 March 2015
Available online 7 April 2015

Keywords:
Glycerol
Conversion
Ni/La_2O_3
Acetol
Syngas

ABSTRACT

The current global tendency is to increase the use of biofuels. This tendency has generated an oversupply of glycerol, which is the primary byproduct that is formed during the production of biodiesel. An alternative use for glycerol is based on chemical transformation to high-added-value derivatives at the industrial and/or energy level. During the decomposition of gaseous glycerol, polymers, alcohols and other oxygenated compounds can be generated with a selectivity that depends on the characteristics of the catalyst used. Accordingly, in this work, the acid and base characteristics of the catalyst support and the nickel in the Ni/La_2O_3 were investigated, as well as their influence on selectivity toward acetol at 400 °C and syngas at 700 °C. Generally, it was determined that the use of a basic catalyst support favors glycerol dehydration with respect to the formation of acetol. Moreover, it was found that the nickel particles present in the catalyst increased yield gas fraction at high reaction temperatures with a high selectivity to the syngas.

1. Introduction

Currently, due to the increase in the price of petroleum, the limited resources of fossil fuels and the environmental implications related to their use, there exists a clear tendency toward the increase in the use of alternative fuels; among these, the production of biodiesel has increased significantly in recent years [1]. As a consequence, this has brought about the oversupply of glycerol, which is the primary sub-product generated during biodiesel production. One alternative use of glycerol involves its chemical transformation into derivatives of high added value at the industrial scale [2–6]. For example, a recent comparison for a fossil- and renewable-based route for 1,2-propanediol production showed that the renewable-based routes can provide a viable alternative to the petrochemical route and both approaches must therefore be considered in a global process [7].

In this type of process, catalysis is of great importance, given that the reaction selectivity increases with respect to certain products, depending on the catalyst characteristics [8]. In this sense, basic catalysts, such as rare-earth oxides (La_2O_3, Pr_6O_{11}, Nd_2O_3), among others, have shown high catalytic activity toward the dehydration of alcohols, such as 1,3-butanediol, 1,4-butanediol and glycerol; (conversions above 80% have been reported for La_2O_3) [9–11]. This has been attributed to the basic character of the catalyst (the strength and quantity of the active sites); accordingly, it can expect that the use of light rare-earth oxides (REOS) could favor the formation of glycerol-dehydration products due to their strong basicity [12].

Moreover, some studies have shown that metallic catalysts are a good alternative for glycerol decomposition via reforming, showing high selectivity toward the formation of hydrogen [13–15]. In this case, although various authors have suggested that nickel catalysts maximize hydrogen production from glycerol, their use has been equally associated with the formation of carbonaceous residues that cause catalyst deactivation [16–18]. One of the alternatives for counteracting this effect is the use of mixed oxides as catalytic precursors; for example, the perovskite $LaNiO_3$. Ni/La_2O_3 catalysts composed of metallic nanoparticles highly dispersed on the surface of the support have been generated from this material. This type of catalyst has shown high activity and stability during methane reforming reactions, which could be extended to glycerol reforming reactions [19,20].

Hernandez et al. [21] reported that the basic catalysts La_2O_3 and Ni/La_2O_3 can both be used to produce added value products such as acetol by glycerol dehydration. In the present work, the objective was to establish the acid–base properties of Ni/La_2O_3 and its effect in the catalytic activity of the glycerol decomposition reaction at 400 °C. The acid–base properties of La_2O_3 and its catalytic

* Corresponding author. Tel.: +57 4 2196611; fax: +57 4 2191073.
E-mail address: john.fernandez@udea.edu.co (J.J. Fernández).

http://dx.doi.org/10.1016/j.apcata.2015.03.045
0926-860X/

effect were determined, in comparison to a commercial catalyst, i.e., γ-alumina, which displays a predominantly acidic character even though it possess both acidic and basic sites [22,23].

2. Experimental

2.1. Preparation of the catalysts

Lanthanum oxide (La_2O_3) and the perovskite $LaNiO_3$ were prepared by the auto-combustion method, following the procedure reported in previous works from our research group [19,20]. Following this method, an equimolar solution was prepared from metal nitrates and glycine ($H_2NCH_2CO_2H$) was used as an ignition promoter, at a ratio of $NO_3^-/NH_2 = 1$, in which water was evaporated at 90 °C until the formation of a gel. Subsequently, this gel was taken to the temperature at which auto-combustion occurs (approximately 250 °C), which is an exothermic process and is responsible for the combustion of carbonaceous material and the formation of a metal oxide. To eliminate the fraction of carbonaceous compounds that remain in the metal oxide, calcination was carried out at 700 °C in an oxidizing atmosphere for 6 h with the goal of removing the carbon present in the solid and forming the perovskite-type crystalline phase, $LaNiO_3$ (the nickel nominal content was 23.8% by weight). The Ni/La_2O_3 catalyst was obtained by in situ reduction of the $LaNiO_3$ perovskite at 700 °C prior to the start of the reaction.

2.2. Characterization of the catalysts

The La_2O_3 and Ni/La_2O_3 catalysts were characterized by X-ray diffraction (XRD) using a Panalytical X'PERT PRO MPD powder X-ray diffractometer equipped with a copper anode (Cu Kα1 = 1.5406 Å). The equipment was operated at 45 kV and 40 mA, and data acquisition was carried out for an angle 2θ between 10 and 90°, with a step size of 0.01° and an acquisition time of 1 s/step. The mesh parameters were determined with a step size of 0.01° and an acquisition time of 2 s/step. The experimental diffractograms were compared with the Power Diffraction File (PDF) database.

The determination of the number of acidic and basic sites in the Ni/La_2O_3, La_2O_3, and γ-Al_2O_3 catalysts was carried out via the temperature programmed desorption (TPD) of NH_3 and CO_2, respectively, these experiments were carried out in a Micromeritics Autochem II using a thermal conductivity detector (TCD). Before carrying out the TPD experiments, the catalysts were first subjected to a pre-treatment in helium at 400 °C for 1 h.

In the case of the TPD experiments with NH_3 (TPD NH_3), after cooling the system to 50 °C, each catalyst was subjected to an NH_3 flow (0.3% in helium) for 90 min; after purging the system in helium for 30 min, a thermal treatment in helium from 50 °C to 1000 °C was performed, using a ramp rate of 10 °C/min and then holding at this temperature for 30 min. The adsorption of CO_2 was performed at 50 °C, for which each catalyst was subjected to a pure CO_2 flow for 90 min. Subsequently, the system was purged under He flow for 30 min. The desorption of CO_2 was performed under He flow while increasing the temperature from 50 °C to 850 °C, using a ramp rate of 10 °C/min; at this temperature, an isothermal hold was carried out for 1 h.

The moles of desorbed NH_3 and CO_2 were calculated via the integration of the thermogram signals and then were related to the areas obtained for known volumes of each gas analyzed at standard conditions, for which the deconvolution of the areas was carried out by assuming a Gaussian distribution (with a correlation index of 99%). The results obtained were normalized per gram of catalyst.

Additionally, the surface acidic sites of the supports were characterized by pyridine adsorption–desorption experiment using infrared spectroscopy technique. The experiments were carried out in a Nexus Nicolet spectrometer equipped with a high temperature transmission cell and a DTGS detector, spectra were recorded with a resolution of 4 cm^{-1} and 64 scans. The oxide powder was pressed into self-supported wafer (2 cm diameter) mounted into the cell and degassed overnight at 700 °C under vacuum. Then pyridine vapor was adsorbed by the sample at room temperature, after that the excess of pyridine was eliminated from the system using vacuum. FTIR spectra were recorded after pyridine desorption at different temperatures.

2.3. Catalytic tests

The decomposition of pure glycerol was carried out in a fixed bed reactor at atmospheric pressure, which can be seen in Fig. 1. During the reaction, a continuous flow of pure glycerol (99.9%) was passed through the vaporizer before the reactor. The vaporizer was hold at 290 °C and the reactor temperature varied between 400 °C and 700 °C. The glycerol/argon ratio was 20/80 during all experiments. The catalytic tests were carried out using 20 mg of catalyst.

During the reaction time (2.5 h), the gases were identified online, using a quadrupole mass analyzer (Pfeiffer QMS 200) in which the evolution of syngas was evaluated. In the case of liquid-phase products, the condensates were recovered in a water-ice trap during the reaction. Product separation and quantification were performed using an Agilent 6890 gas chromatograph equipped with a DB-FFAP column (60 m × 0.25 mm × 0.25 μm) and FID detector. For product quantification, butanol was used as the internal standard. Generally, all of the runs carried out in GC to identify and quantify the compounds were performed by triplicate. In the case of the catalytic tests, the reactions were performed by duplicate in order to guarantee the reproducibility of the results.

Conversion of glycerol and product selectivity in the liquid phase was calculated according to the following equations:

$$\text{Glycerol conversion}\,(\%) = \frac{\text{weight of glycerol reacted}}{\text{weight of glycerol in the feed}} \times 100$$

$$\text{Product } i \text{ Selectivity}\,(\%) = \frac{\text{weight of } i \text{ product}}{\text{weight of liquid fraction}} \times 100$$

3. Results and discussion

3.1. Properties of the catalysts

The presence of the metallic nickel and lanthanum oxide phases in the structure of the Ni/La_2O_3 catalyst prepared by reduction of $LaNiO_3$ perovskite at 700 °C was corroborated by XRD (Fig. 2), which is in agreement with previous studies, where the experimental conditions for achieving the reduction (under H_2 atmosphere at 700 °C) ensured the complete destruction of the perovskite structure [20–24]. Meanwhile, the measurement of nickel oxidation state using XPS analysis, reported in our recent paper, indicates that the reduction of $LaNiO_3$ perovskite at 700 °C allows to obtain only metallic nickel (100% Ni^0 on the catalyst surface) [21].

With the purpose to evaluate the acid–base properties of the La_2O_3 and Ni/La_2O_3 catalysts, Table 1 shows the TPD results for the

Table 1
The acid–base properties of the different catalysts.

	Al_2O_3 [a]	La_2O_3	Ni/La_2O_3
BET area (m^2/g)	80	10	12
Total number of acidic sites (μmoles NH_3/g)	609	115	69
Total number of basic sites (μmoles CO_2/g)	289	511	342

[a] γ Al_2O_3 Alfa Aesar, 99.97%.

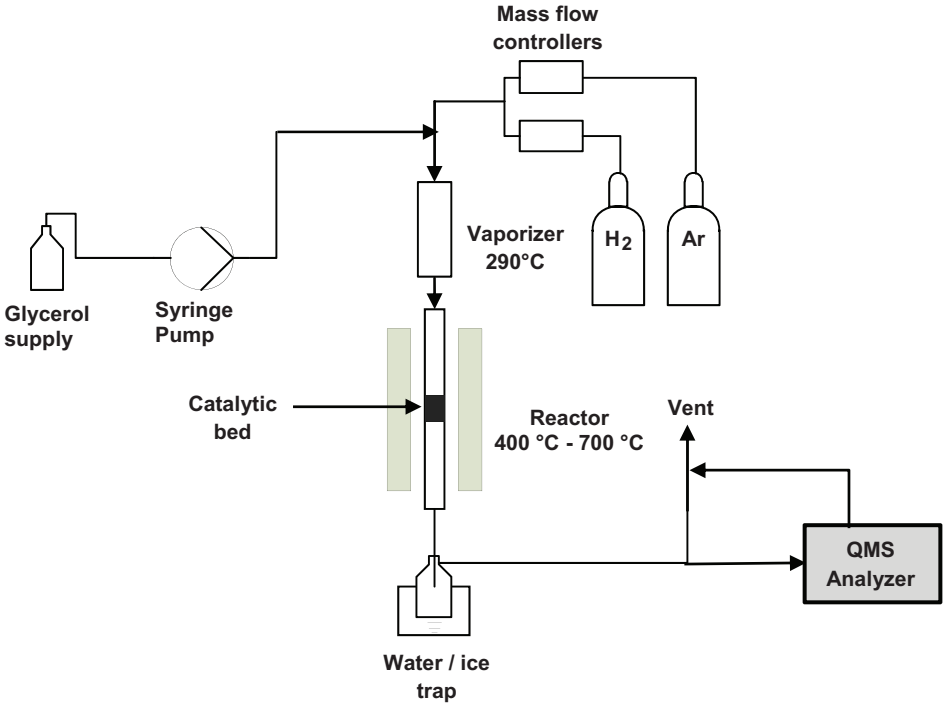

Fig. 1. The experimental set-up.

NH_3 and CO_2 test molecules on these materials, and the comparison with a commercial catalyst (γ-Alumina Alfa – Aesar) whose acid–base characteristics are known [22,23]. The results indicate the highly basic character of La_2O_3 and Ni/La_2O_3 prepared from the perovskite $LaNiO_3$ and the strongly acidic character of the alumina.

The distribution of basic sites in the catalysts was evaluated based on the desorption profiles (TPD CO_2), as is shown in Fig. 3, and it was found that both Ni/La_2O_3 and La_2O_3 displayed significant heterogeneity in basic sites, showing only a single desorption at temperatures below 450 °C (with a maximum at 373 °C) for La_2O_3. In contrast, for Ni/La_2O_3, two desorption peaks were observed (with maxima at 401 °C and 419 °C, respectively). However, the relative proportion of species in the catalysts, associated with the formation of bicarbonates in weak OH^- and O^{2-} species, is greater in La_2O_3 with respect to Ni/La_2O_3 (Table 1). Additionally, the peaks at temperatures above 450 °C observed in both catalyst correspond to CO_2 desorption, which is associated with the presence of monodentate and polydentate carbonates species [12,25], though the type of species and amount are different on La_2O_3 with respect to Ni/La_2O_3 as observed for adsorption sites at lower temperatures; suggesting that the Ni–La_2O_3 interactions significantly modified the surface properties of the support. In the case of γ-Al_2O_3 (no showed), only one desorption peak of weak species is present in relation to La_2O_3 and Ni/La_2O_3, which is consistent with previous reports in the literature [23].

Regarding the acidic properties, Fig. 4 shows the NH_3 TPD with the distribution of acidic sites in the tested catalysts. In this figure it is important to highlight in the case of γ-alumina (Fig. 4c), the NH_3 desorption behavior at low and moderate temperatures, which can be attributed to the presence of acidic sites of weak and moderate character (with maxima at 142 °C and 380 °C) in agreement with the literature reports. These results demonstrate the prevailing acidic character of this material. Concerning La_2O_3 (Fig. 4b), two NH_3 desorption peaks with maxima at 317 °C and 436 °C (moderately acidic sites) are observed, which indicates two types of sites with different acidic strength. It is important to highlight that the presence of Ni caused the formation of new weakly acidic sites (with a maximum at 142 °C), in addition to the formation of a unique type of moderately acidic site (with a maximum at 420 °C). This result could be related to interactions between the support and the active phase that can occur in this catalyst as could

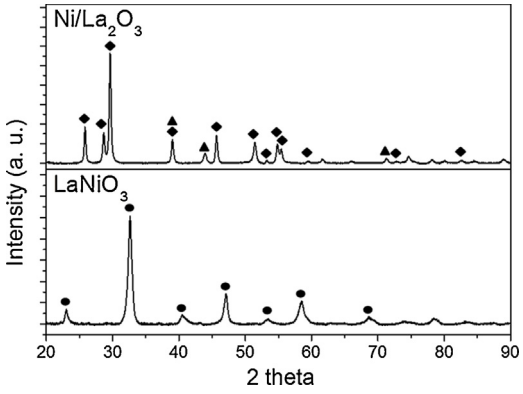

Fig. 2. XRD of the $LaNiO_3$ and Ni/La_2O_3 catalyst after in situ reduction of $LaNiO_3$ at 700 °C (•) $LaNiO_3$ (PDF 00-88-0633), (♦) La_2O_3 (PDF 01-083-1349), (▲) Ni^0 (PDF 00-045-1027).

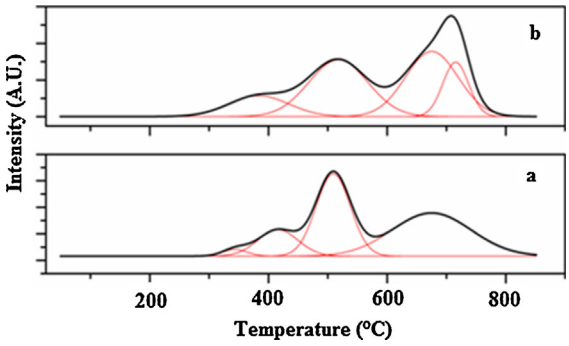

Fig. 3. The CO_2 TPD profiles for Ni/La_2O_3 (a), La_2O_3 (b).

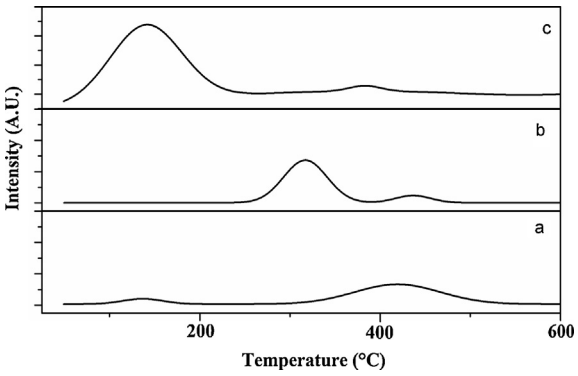

Fig. 4. The NH_3 TPD profiles for Ni/La_2O_3 (a), La_2O_3 (b) and Al_2O_3 (c).

be seen in the case of basic sites evaluated via TPD of CO_2, suggesting in addition that such interaction occurs selectively, that is, the Ni interacts with La_2O_3 through acidic sites of intermediate strength.

Taking into account all of the above, it is possible to conclude that the basic character of the studied catalysts (as a function of the number of basic sites evaluated) followed the trend γ-Al_2O_3 < Ni/La_2O_3 < La_2O_3, for which the number of basic sites in the catalyst Ni/La_2O_3 decreased with respect to La_2O_3, possibly because of the strong interaction between nickel and the La_2O_3. Regarding the acidic character of the evaluated catalysts, the trend of Ni/La_2O_3 < La_2O_3 < γ Al_2O_3 was found, which corroborated the strong effect of the metal–support interaction on the acid–base characteristics of the catalyst. It is important to highlight that, in the case of alumina, although the catalyst showed a high NH_3 desorption, indicating a strongly acidic character, it equally exhibits a significant number of basic sites, given that the amount of desorbed CO_2 is comparable to that of the catalyst Ni/La_2O_3 and more than half of the value obtained for La_2O_3.

The surface acidic properties for the supports were further evaluated by FTIR analyses of adsorbed pyridine. Upon pyridine adsorption at room temperature, the FTIR spectra were collected after desorption at different temperatures. Fig. 5 shows the difference spectra of the samples in the pyridine ring vibration region.

In Fig. 5a characteristics absorption bands of pyridine at 1623/1618, 1577, 1493 and 1452 cm^{-1} on γ-Al_2O_3 sample were observed [26–30]; indicating the presence of different types of Lewis acidic sites with different strength [31]. For La_2O_3, absorption bands of pyridine were also observed at 1603, 1582, 1545, 1479/1474, 1439 cm^{-1}; the absorption band centered at 1545 cm^{-1} could indicate the presence of Bronsted acidic sites on La_2O_3 surface to protonate pyridine.

In Fig. 5b, the amount of adsorbed pyridine was estimated by integrating the absorption band at ~1452 cm^{-1} (ν_{19b}) using its molar coefficient ($\varepsilon_{\nu 19b}$ = 1.3 cm μmol^{-1}) [28,29,32]. This figure shows that the amount of acidic Lewis sites in the γ-Al_2O_3 is largely superior to the amount obtained for La_2O_3. γ-Al_2O_3 exhibits LAS sufficiently strong for retaining pyridine adsorbed at elevated temperatures.

Table 2
The identified products generated during the glycerol decomposition reaction.

Fraction	Identified products
Liquid fraction	CH_3OH (methanol), C_2H_5OH (ethanol), $HOCH_2(OH)CHCH_3$ (1,2-propanediol), $HO(CH_2)_3OH$ (1,3-propanediol), CH_3CHO (acetaldehyde), CH_2=$CHCHO$ (acrolein), CH_3COOH (acetic acid), C_2H_5COOH (propionic acid), $CH_3C(O)CH_3$ (acetone), $CH_3C(O)CH_2OH$ (hydroxyacetone).
Gaseous fraction	H_2 (hydrogen), CO (carbon monoxide), CO_2 (carbon dioxide), CH_4 (methane), C_2H_4 (ethylene), C_2H_6 (ethane)
Solid fraction	Carbonaceous material (coke)

3.2. Identification of the reaction products

During the catalytic decomposition reaction of glycerol at 400 °C, various products distributed in different fractions were obtained, including a liquid fraction, primarily comprising condensable oxygenated compounds, a gaseous fraction, and a solid fraction, composed of carbonaceous material generated during the reaction. The products that were identified are shown in Table 2.

These results are in agreement with Eq. (1), which shows the general glycerol decomposition reaction [33].

$$C_3H_8O_{3(l)} \rightarrow C_xH_yO_{z(l,g)} + (H_2, CO, CO_2, CH_4, \ldots)_{(g)} + C_{(s)} \quad (1)$$

3.3. Effects of metallic Ni and the acid–base properties of the catalyst

In order to study the effects of metallic nickel and the acid–base properties of the Ni/La_2O_3, on its catalytic activity during glycerol decomposition at 400 °C, the results of a catalytic test were compared to the results obtained for La_2O_3, whose character is predominantly basic, and for the alumina, which, although it displayed moderately basic sites, showed a prevailing acidic character.

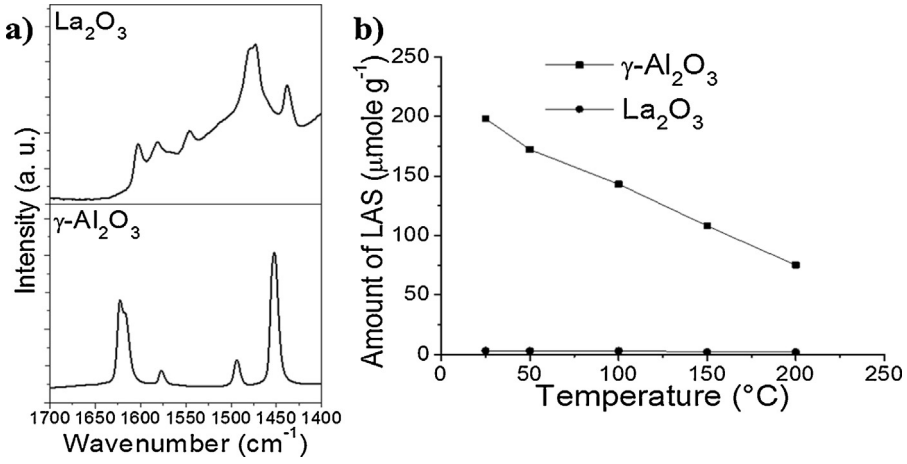

Fig. 5. (a) FTIR spectra of pyridine adsorbed on γ-Al_2O_3 and La_2O_3 after desorption at 150 °C, (b) amount of Lewis acidic sites (LAS) on γ-Al_2O_3 and La_2O_3.

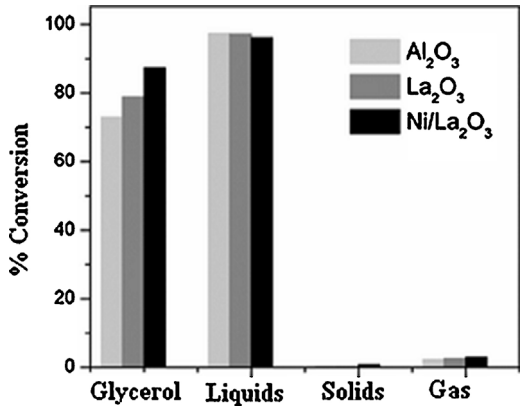

Fig. 6. Effect of the nature of the catalyst on glycerol conversion toward different fractions during glycerol decomposition at 400 °C.

Regarding glycerol conversion, Fig. 6 shows that, independently of the type of catalyst used during the reaction, there is a high selectivity toward products pertaining to the liquid fraction (above 96% in all cases) in addition to the low formation of gases and carbonaceous material because the reactions of dehydration and partial decomposition of glycerol are primarily favored at 400 °C. In turn, the increase in glycerol conversion when using the catalyst with nickel confirmed that the presence of this metal favors cracking of the glycerol molecule, as has been reported in the literature [34].

Moreover, due to the large quantity of products in the liquid fraction that were obtained at 400 °C, the selectivity toward specific products from this fraction was evaluated at this temperature (as shown in Table 3). Generally, it was found that the selectivity toward acetol is influenced by the basic characteristics of the catalyst, according to the trend $Al_2O_3 < Ni/La_2O_3 < La_2O_3$. Additionally, Table 3 shows that the formation of polymers has an inverse trend, That is, the formation of polymers was influenced by the acidic properties of the catalyst and followed the trend of $Al_2O_3 > Ni/La_2O_3 > La_2O_3$.

From the analysis of these results, it is possible to infer that the use of lanthanum oxide as a catalyst favored the route of partial glycerol decomposition toward the formation of acetol and, consequently, toward the formation of 1,2-propanediol; this compound can be produced through a two-step process, where glycerol is first dehydrated to acetol which is subsequently hydrogenated to 1,2-Propanediol. The solid catalysts active for the reaction usually are composed of bi-functional metal–acid catalysts, which combine acid sites for dehydration reactions (like ZnO, C, Rh, SiO_2, Al_2O_3) and metal sites for hydrogenation reactions (such as Cu, Pd, Rh, Ni). Best results are obtained by using noble metals, because their presence promotes the subsequent hydrogenation of acetol [7,21,35].

Table 3
Products composition of the liquid fraction obtained during the catalytic decomposition of glycerol at 400 °C.

Catalyst	X_L (%)	Selectivity to products in the liquid phase (%)				
		Water	Acetol[a]	1,2-Prop[b]	Polym[c]	Others[d]
La_2O_3	97.2	10.3	59.6	7.9	18.5	3.7
Al_2O_3	97.5	16.8	30.9	4.2	46.5	1.6
Ni/La_2O_3	96.8	6.0	39.9	7.0	35.9	11.2

[a] Acetol
[b] 1,2-Propanediol.
[c] Polymers of glycerol.
[d] Others: acetaldehyde, acetone, acrolein, methanol, ethanol, acetic acid, propanoic acid.

Analyzing the products identified via this route, it was possible to establish the primary presence of highly oxygenated polymers, such as glycerol- and acetol-based oligomers. However, it was found that acetol formation decreased by utilizing Ni/La_2O_3 as a catalyst, and at the same time, the amount of oxygenated light compounds present in the liquid phase and the amount of polymers generated from these compounds increased.

The use of alumina (Al_2O_3) as catalyst showed a significant decrease in the formation of acetol. In turn, the formation of polymers and the presence of water in the liquid phase increased significantly, which can be related to the greater formation of acrolein as the intermediate product [8]. Acrolein reacted to cause the formation of polymers via condensation reactions, which could explain the simultaneous increase in the production of water. In this case, in addition to the polymers generated from acrolein, polymers generated from glycerol and acetol also were identified in the liquid phase.

Based on the above mentioned discussion and considering the results found in the literature, which suggest that catalysts with acidic characteristics favor the glycerol dehydration route toward the formation of acrolein [8,36,37], in this study, it is suggested that the formation of acetol from glycerol dehydration is directly related to the acid–base properties of the catalyst support. Although the presence of Bronsted sites has been associated in the literature with a greater selectivity toward the dehydration product (acrolein) [38,39], in La_2O_3 the negligible amount of acidic sites observed in Fig. 5b explains the absence of acrolein in the liquid phase using this catalyst. Instead, high selectivity to acetol is achieved which has been associated with the basic character of La_2O_3 catalyst support. For the case of catalysts such as alumina, which has potentially catalytic acidic and basic sites in its structure, it has been found that the dehydration mechanisms occur by means of a concerted reaction on the basic sites and on Lewis-acid sites present in the structure [23].

For catalysts with a strongly basic character, such as La_2O_3, it is proposed that the glycerol dehydration reaction occurs via the E1cB mechanism, which involves the formation of a carbanion. Accordingly, it was found that this type of catalyst promotes the formation of products through Hoffman elimination, possibly because in this case, the primary hydroxyl groups are the least impeded and thus the most reactive [12].

Concerning the formation of acetol from glycerol, previous reports have suggested that glycerol hydrogenolysis occurs prior to the dehydration mechanism, generating glyceraldehyde as an intermediate product. These dehydrogenation–dehydration and hydrogenation mechanisms are both justified by the presence of a catalyst with a strongly basic character, as is the case of La_2O_3 [40].

Due to the strongly basic character found for the Ni/La_2O_3 catalyst, it is possible to infer that glycerol dehydration with this catalyst occurs via the E1cB mechanism, which explains the high selectivity toward acetol formation. However, it is also proposed that the presence of the nickel metallic sites favored, to a certain degree, the cracking of both glycerol and some dehydration intermediaries into smaller molecules, which accounts for the increase in the selectivity toward lighter oxygenated compounds. Such compounds can be polymerized easily due to the basic characteristics of the catalyst, as has already been reported in some publications [41,42]. This effect becomes more evident upon increasing the reaction temperature, as shown in Fig. 7. It can be seen that at 700 °C, the conversion to gaseous products exceeds 80%, with hydrogen and carbon monoxide being the primary products that are generated in this fraction.

With regard to the composition of the syngas as a function of temperature, it was found that by increasing the temperature, the formation of CO was favored. Meanwhile, the ratio of H_2/CO

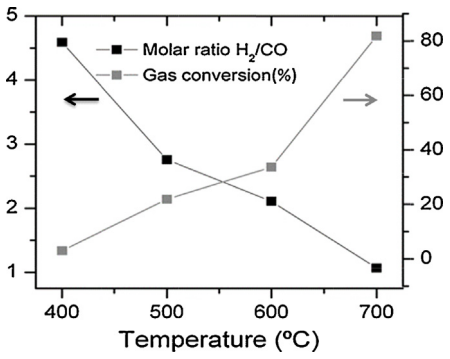

Fig. 7. The effect of temperature on the ratio of syngas.

changed from about 4 at 400 °C to about 1 at 700 °C. The latter being the optimal ratio of H_2/CO in Fischer Tropsch processes for obtaining long-chain hydrocarbons [43].

The role of temperature in these reactions has been evaluated from a thermodynamic viewpoint. Moderated temperatures (about 400 °C) favor the hydrogen production from glycerol decomposition as well as the water shift reaction, because the presence of water generated in situ during the glycerol dehydration at these temperatures. On the other hand, although high temperatures favor the formation of hydrogen due to the reforming reaction of glycerol, the ratio of H_2/CO decreases with increasing temperature, due to the increased production of CO, which is explained considering the reverse water shift reaction promoted by the reducing atmosphere, due to presence of large amount of hydrogen and high temperatures [17,44]. Despite this, it is important to note that although such studies have concluded that high temperatures and low pressures favor hydrogen production, the thermodynamic analysis is restricted only to the primary products of decomposition of glycerol (H_2, CO, CO_2 and CO_2) [45].

In this case, the good selectivity toward the formation of syngas at high temperatures was related to the use of Ni/La_2O_3 as the catalyst, which favored the cracking reactions of glycerol and its intermediaries due to the presence of nickel particles dispersed on the catalyst support, which acted as active sites on the catalyst. The catalytic effect of nickel in this type of reaction has been demonstrated in previous studies of glycerol reforming, in which high selectivity toward hydrogen formation was obtained [34].

4. Conclusions

The present study showed that the acetol formation from glycerol catalytic dehydration is mostly related to the strongly basic character of the catalyst. In this sense, it was found that at 400 °C a catalyst such as alumina, which mainly acidic, favored the glycerol dehydration route to acrolein and acrolein polymers, while the La_2O_3 catalysts with predominantly basic sites direct the glycerol dehydration toward acetol. On the other hand, the presence of Ni supported on basic surface (Ni/La_2O_3) resulted in the increased cleavage of C-C bonds of the glycerol molecule. Consequently, the cracking increased with reaction temperature, favoring the glycerol reforming reaction at 700 °C, and leading to syngas formation with an optimum H_2/CO ratio for Fischer Tropsch synthesis.

Acknowledgements

The authors thank the Ministry of Agriculture and Rural Development of Colombia (MADR project 20X07D3347-498) and the Universidad de Antioquia (Programa de Sostenibilidad 2014–2015) for financial support. Diana Hernández thanks COLCIENCIAS for the doctoral scholarship.

References

[1] R. Adib, Renewables 2011 Global Status Report, Renewable Energy Policy Network for the 21st Century, 2011.
[2] S. Bagheri, N.M. Julkapli, W.A. Yehye, Renew. Sustain. Energy Rev. 41 (2015) 113–127.
[3] M. Pagliaro, R. Ciriminna, H. Kimura, M. Rossi, C. Della Pina, Angew. Chem. Int. Ed. 46 (2007) 4434–4440.
[4] D.T. Johnson, K.A. Taconi, Environ. Prog. 26 (2007) 338–348.
[5] A. Behr, J. Eilting, K. Irawadi, J. Leschinski, F. Lindner, Green Chem. 10 (2008) 13–30.
[6] C.-H. Zhou, J.N. Beltramini, Y.-X. Fan, G.Q. Lu, Chem. Soc. Rev. 37 (2008) 527–549.
[7] V. Montes, M. Checa, A. Marinas, M. Boutonnet, J.M. Marinas, F.J. Urbano, S. Järas, C. Pinel, Catal. Today 223 (2014) 129–137.
[8] H. Atia, U. Armbruster, A. Martin, J. Catal. 258 (2008) 71–82.
[9] S. Sato, R. Takahashi, M. Kobune, H. Inoue, Y. Izawa, H. Ohno, K. Takahashi, Appl. Catal. A: Gen. 356 (2009) 64–71.
[10] S. Sato, R. Takahashi, T. Sodesawa, A. Igarashi, H. Inoue, Appl. Catal. A: Gen. 328 (2007) 109–116.
[11] M. Velasquez, A. Santamaria, C. Batiot-Dupeyrat, Appl. Catal. B: Environ. 160–161 (2014) 606–613.
[12] S. Sato, R. Takahashi, M. Kobune, H. Gotoh, Appl. Catal. A: Gen. 356 (2009) 57–63.
[13] M. Pagliaro, M. Rossi, The Future of Glycerol, 2nd ed., The Royal Society of Chemistry, 2010, pp. 29–44.
[14] S. Adhikari, S. Fernando, S. Gwaltney, S.D. Filip To, R.M. Bricka, P.H. Steele, A. Haryanto, Int. J. Hydrogen Energy 32 (2007) 2875–2880.
[15] R.R. Davda, J.W. Shabaker, G.W. Huber, R.D. Cortright, J.A. Dumesic, Appl. Catal. B: Environ. 56 (2005) 171–186.
[16] A. Iriondo, V.L. Barrio, J.F. Cambra, P.L. Arias, M.B. Güemez, R.M. Navarro, M.C. Sánchez-Sánchez, J.L.G. Fierro, Top. Catal. 49 (2008) 46–58.
[17] V. Nichele, M. Signoretto, F. Menegazzo, A. Gallo, V. Dal Santo, G. Cruciani, G. Cerrato, Appl. Catal. B: Environ. 111–112 (2012) 225–232.
[18] M.H. Youn, J.G. Seo, H. Lee, Y. Bang, J.S. Chung, I.K. Song, Appl. Catal. B: Environ. 98 (2010) 57–64.
[19] G. Sierra, C. Batiot-Dupeyrat, J. Barrault, E. Florez, F. Mondragón, Appl. Catal. A: Gen. 334 (2008) 251–258.
[20] G. Sierra, J. Barrault, C. Batiot-Dupeyrat, F. Mondragón, Catal. Today 149 (2010) 365–371.
[21] D. Hernandez, M. Velasquez, P. Ayrault, D. Lopez, J.J. Fernandez, A. Santamaria, C. Batiot-Dupeyrat, Appl. Catal. A: Gen. 467 (2013) 315–324.
[22] M. Kaltchev, W.T. Tysoe, Surf. Sci. 430 (1999) 29–36.
[23] S. Carre, B. Tapin, N.S. Gnep, R. Revel, P. Magnoux, Appl. Catal. A: Gen. 372 (2010) 26–33.
[24] G.S. Gallego, F. Mondragón, J. Barrault, J.-M. Tatibouët, C. Batiot-Dupeyrat, Appl. Catal. A: Gen. 311 (2006) 164–171.
[25] O.V. Manoilova, S.G. Podkolzin, B. Tope, J. Lercher, E.E. Stangland, J.-M. Goupil, B.M. Weckhuysen, J. Phys. Chem. B 108 (2004) 15770–15781.
[26] E.P. Parry, J. Catal. 2 (1963) 371–379.
[27] C. Morterra, A. Chiorino, G. Ghiotti, E. Garrone, J. Chem. Soc. Faraday Trans. 1: Phys. Chem. Condensed Phases 75 (1979) 271–288.
[28] F. Can, A. Flura, X. Courtois, S. Royer, G. Blanchard, P. Marécot, D. Duprez, Catal. Today 164 (2011) 474–479.
[29] F. Can, A. Le Valant, N. Bion, F. Epron, D. Duprez, J. Phys. Chem. C 112 (2008) 14145–14153.
[30] X. Liu, J. Phys. Chem. C 112 (2008) 5066–5073.
[31] X. Liu, R.E. Truitt, J. Am. Chem. Soc. 119 (1997) 9856–9860.
[32] S. Khabtou, T. Chevreau, J.C. Lavalley, Microporous Mater. 3 (1994) 133–148.
[33] T. Valliyappan, N.N. Bakhshi, A.K. Dalai, Bioresour. Technol. 99 (2008) 4476–4483.
[34] E. Chornet, S. Czernik, Nature 418 (2002) 928–929.
[35] I. Gandarias, P.L. Arias, J. Requies, M.B. Güemez, J.L.G. Fierro, Appl. Catal. B: Environ. 97 (2010) 248–256.
[36] E. Kraleva, R. Palcheva, L. Dimitrov, U. Armbruster, A. Brückner, A. Spojakina, J. Mater. Sci. 46 (2011) 7160–7168.
[37] W. Suprun, M. Lutecki, T. Haber, H. Papp, J. Mol. Catal. A: Chem. 309 (2009) 71–78.
[38] C.L. Lima, S.J.S. Vasconcelos, J.M. Filho, B.C. Neto, M.G.C. Rocha, P. Bargiela, A.C. Oliveira, Appl. Catal. A: Gen. 399 (2011) 50–62.
[39] A. Alhanash, E.F. Kozhevnikova, I.V. Kozhevnikov, Appl. Catal. A: Gen. 378 (2010) 11–18.
[40] R.B. Mane, C.V. Rode, Org. Process Res. Dev. 16 (2012) 1043–1052.
[41] J. Barrault, J.M. Clacens, Y. Pouilloux, Top. Catal. 27 (2004) 137–142.
[42] A. Martin, M. Richter, Eur. J. Lipid Sci. Technol. 113 (2011) 100–117.
[43] D. Mark E, Catal. Today 71 (2002) 227–241.
[44] I.N. Buffoni, F. Pompeo, G.F. Santori, N.N. Nichio, Catal. Commun. 10 (2009) 1656–1660.
[45] S. Adhikari, S.D. Fernando, A. Haryanto, Energy Convers. Manage. 50 (2009) 2600–2604.